J Rec Const Resources 2(4)297-306(2014)
http://dx.doi.org/10.14190/JRCR.2014.2.4.297

Print ISSN : 2288-3320
Online ISSN : 2288-369X

Durability Enhancement in Nano-Silica Admixed Reinforced Mortar

Velu Saraswathy[1] · Subbiah Karthick[1] · Seung-Jun Kwon[2]*

(Received November 5, 2014 / Revised December 4, 2014 / Accepted December 11, 2014)

Recently nano-materials are gaining more importance in the construction industry due to its enhanced energy efficiency, durability, economy, and sustainability. Nano-silica addition to cement based materials can control the degradation of the fundamental calcium-silicate-hydrate reaction of concrete caused by calcium leaching in water as well as block water penetration and therefore lead to improvements in durability. In this paper, the influence of synthesized nano silica from locally available rice husk on the mechanical properties and corrosion resistant properties of OPC (Ordinary Portland Cement) has been studied by conducting various experimental investigations. Micro structural properties have been assessed by conducting Scanning Electron Microscopy, Thermo gravimetry and Differential Thermal Analysis, X-Ray Diffraction analysis, and FTIR studies. The experimental results revealed that NS reacted with calcium hydroxide crystals in the cement paste and produces Calcium Silicate Hydrate gel which enhanced the strength and acts as a filler which filled the nano pores present in concrete. Hence the strength and corrosion resistant properties were enhanced than the control.

Keywords : Nano silica, Chloride penetration, EIS, SEM, TGA, XRD, FTIR

1. INTRODUCTION

Durability of concrete structures in marine environment has attracted a lot of attention from many researchers, because it has critical influence on the service life of concrete structures. The uses of mineral admixtures such as Silica fume (SF), fly ash are well recognized to enhance the properties of concrete (Hassan et al. 2000; Memon et al. 2002; Tasdemir, 2003; Gonen and Yazicioglu, 2007; Shannag, 2011). Silica induces the pozzolanic reaction that results in a reduction of the amount of calcium hydroxide in concrete and silica fume reduces the porosity and improves the durability (Constantinides and Ulm 2004).

Recently nano particles become increasing attention and has been applied in many fields to fabricate new materials with novelty function due to their unique physical and chemical properties. The majority of recent nano technology research in construction has focused on the structure of cement based materials and their future mechanisms. The pozzolanic activity of nano–SiO_2 is more obvious than that of silica fume. Nano–SiO_2 can react with calcium hydroxide crystals which are arrayed in the interfacial transition zone (ITZ) between hardened cement paste and aggregates produce C–S–H gel. The size and amount of calcium hydroxide crystals are significantly decreased and the early age strength of hardened cement paste is increased (Ye 2001; Chen and Ye 2002; Ye et al. 2003; Sobolev and Ferrara 2005). The incorporation of nano–SiO_2 can improve the resistance of water penetration through concrete (Ji 2005). Mondal et al. (2010) has reported that samples with NS had almost twice the amount of high stiffness C–S–H as the samples with silica fume (Mondal et al. 2010). Addition of NS (Nano–SiO_2) in cement paste and concrete can result in

* Corresponding author E-mail: jjuni98@hannam.ac.kr

[1]Corrosion Protection Division, Central Electrochemical Research Institute, India
[2]Hannam University, Civil and Environmental Eng., Daejeon, 306–791, Korea

different effects and the accelerating effect in cement paste is well reported by several authors. Bjornstrom et al. (2004) has reported the accelerating effects of colloidal NS CS (Colloidal Silica) accelerates the dissolution of the Ca_3SiO_5 (C_3S) phase and renders a more rapid formation of C-S-H binding phase (Qing et al. 2007; Lin et al. 2008; Senff et al. 2009; Li et al. 2004; Khanzadi et al. 2010; Ranjbar and Rastegar 2009). Gengying has reported that fly ash has low initial activity, but the pozzolanic activity has been significantly increased after incorporating a little nano-SiO_2 (Li 2004). Gaitero et al. (2008) has reported that the calcium leaching is reduced by the addition of silica nano particles with cement paste. Nano silica particles not only have the filler effect but also increase the pozzolanic activity(Givi et al. 2011).

However till today there is no published report on the corrosion resistant properties of the NS admixed concrete. Hence in the present investigation, NS was synthesized from the locally available Rice Husk Ash (RHA) and it was characterized using XRD and SEM / EDAX and evaluated for their mechanical, diffusion and corrosion resistant properties using different approaches.

2. EXPERIMENTAL PROCEDURE

2.1. Material used

2.1.1 Cement used

Ordinary Portland cement (OPC) – 43 Grade as per IS 8112 and locally available rice husk was used for this investigation. Composition of OPC and RHA are given in Table 1.

Table 1. Composition of OPC, RHA, NS

Composition	Weight (%)		
	OPC	RHA	NS
SiO_2	21.0	91.78	98.5
Al_2O_3	5.4	2.22	-
Fe_2O_3	4.6	0.80	-
CaO	63.0	1.27	0.7
MgO	0.7	0.67	-
SO_3	2.8	-	0.2
Na_2O, K_2O and others	-	1.70	
LOI	2.5	1.56	0.6

2.1.2 Synthesis of nano silica

NS synthesized from RHA by precipitation method(Amutha et al. 2010) was used for this investigation. The Synthesized NS was amorphous in nature as evidenced from XRD (Fig. 1) and particle size ranges from 20 to 50nm (Fig. 2). Composition of synthesized NS is given in Table 1 and EDAX (Fig. 3).

2.2 Experimental Methods

2.2.1 Compression Test

The compressive strength of mortar is one of the most

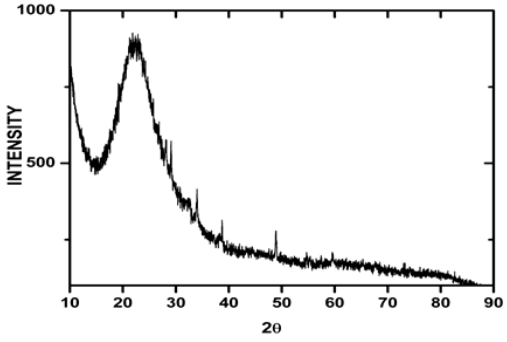

Fig. 1. XRD pattern of synthesized NS

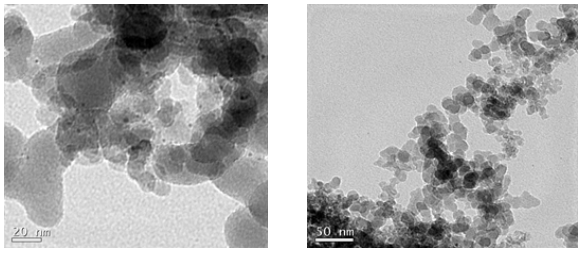

Fig. 2. SEM image of NS

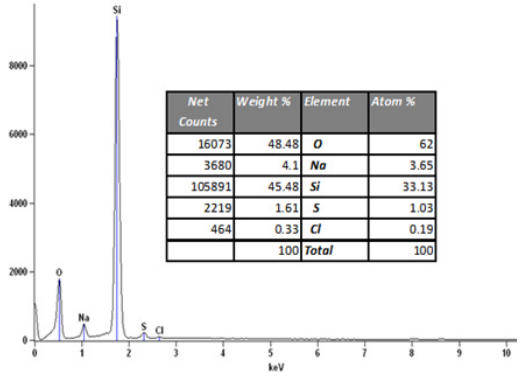

Fig. 3. EDAX results of synthesized NS

important properties for of durability. Mortar specimens of size 100×100×100mm cubes were cast with different types of blended cement mortars. After 24hour, the specimens were demolded and subjected to curing for 28 days in ordinary tap water. After 28 days of curing, the cubes were allowed to become dry for few hours and tested in the compression-testing machine (600KN capacity). The load was applied at the rate of 140kN/min. The ultimate load at which the cube fails was taken for strength determination.

2.2.2 Split tensile test

Split tensile test was carried out as per ASTM C496-90. NS admixed cylindrical mortar of size 60mm diameter and 120mm height were cast using 1:2.75 mortar with W/C (water to cement) ratio of 0.42. During casting, the cylinders were mechanically vibrated using a table vibrator. After 24 hours, the specimens were removed from the mould and subjected to water curing for 28 days. After the specified curing period was over, the mortar cylinders were subjected to split tensile test by using universal testing machine.

2.2.3 Rapid chloride ion penetration test (RCPT)

Chloride penetration is one of the intrinsic properties of concrete to be assessed independently so as to know the long-term durability of concrete structures especially in marine environments. The main mechanism for transport of chloride ions through crack-free concrete is by diffusion. This test was conducted as per ASTM C1202-09. Mortar disc of size 85mm diameter and 50mm thickness with different percentages of NS by weight of cement were cast and allowed to cure for 28 days. After curing, the concrete specimens were subjected to RCPT by impressing 60 V to accelerate the chloride diffusion. When an electric field is applied, movement of chloride ions was due to diffusion and migration. Two halves of the PVC container of diameter 90mm with 100mm long was fixed on both sides of the mortar specimen. One side of the container was filled with 3% NaCl solution and the other side was filled with 0.3N NaOH solution. Titanium Substrate Insoluble Anode (TSIA) was kept immersed on both sides of the container. Compartment containing NaCl was connected to the negative terminal of the power supply and compartment containing NaOH was connected to the positive terminal of the power supply. Current was measured at every 30min up to 6 hours. Chloride contamination and temperature at every 30min was also monitored. Current and time chloride penetration is calculated in terms of coulombs at the end of 6 hours.

2.2.4 Chloride diffusion coefficient

The amount of chloride ion migrating through OPC, OPC with 0.5% to 1.5% NS admixed mortar specimens after 7,14 and 28 days of moisture curing was monitored periodically until steady state was reached (120 hours). Chloride diffusion coefficients were calculated using Nernst-Einstein equation.

$$D = JRTL/[ZFC_0E] \quad (1)$$

Where, D is the chloride diffusion coefficient (m^2/s),J is the flux of chloride ions (mol/m^2s),R is the gas constant (8.314 J/K mol), T is the absolute temperature (300K), L is the thickness of the specimen (m), Z is the valence of chloride ion (Z = 1), F is the Faraday constant (9.648×10^4J/Vmol), C_0 is the initial chloride ion concentration (mol/l), E is the potential applied (60 V).

2.2.5 Impressed voltage test

Cylindrical mortar specimens of size 50mm diameter and 100mm height were cast using 1:2.75 mortar with NS at various percentages containing W/C of 0.42, with centrally embedded rebar of 12mm diameter and 70mm height, containing ordinary Portland cement (control) and NS. During casting, the moulds were mechanically vibrated. After 24 hours, the cylindrical specimens were demolded and allowed to water curing for 28 days and were subjected to impressed voltage test. In this technique, the mortar specimens were immersed in 5% NaCl solution and embedded steel in mortar was made as working electrode with respect to an external stainless steel serving as auxiliary electrode by applying a constant positive potential of 12 V to the system from a DC power source. The variation

of current is recorded with time. For each specimen, the time taken for initial crack and the corresponding maximum anodic current flow was recorded.

2.2.6 Electrochemical Impedance Spectroscopy (EIS)

The same three-electrode cell assembly was used for carrying out EIS. A time interval of 10 to 15 minutes was given for the OCP to reach a steady state value. The impedance measurements were carried out using ACM Instruments, UK. The real part (Z') and imaginary part (-Z") of the cell impedance were measured for various frequencies (30kHz to 10mHz). Plots Z' vs. -Z" were made. Impedance measurements were carried out for steel embedded in OPC and NS admixed mortar.

2.2.7 Potentiodynamic polarization studies

Polarization measurements were carried out to evaluate the corrosion kinetic parameters such as corrosion current (I_{corr}), corrosion potential (E_{corr}), cathodic Tafels lope (b_c) and anodic Tafel slope (b_a). Both cathodic and anodic polarization curves were recorded potentio-dynamically using ACM Instruments, UK. The potentio-dynamic conditions correspond to a potential sweep rate of 10m Vs^{-1} and potential ranges of 0.2 to -0.2V from the OCP. All the experiments were carried out at constant temperature of 32±1℃.

2.2.8 Thermo Gravimetric Analysis (TGA)

NS at different percentages ranging from 0, 0.5, 1.0, 1.5% admixed cement mortar were analyzed by TGA. TGA was performed in a TG Analyzer Model SDT Q600 with a horizontal furnace. It is equipped with an ultra micro balance, which has a resolution of 0.11μg. Aluminium crucibles with 100μl capacity having a pin hole to obtain water vapor self-generated atmosphere were used. The decomposition temperatures of hydrates shift to higher temperature using this type of aluminium crucibles. The gas flow for the surrounding atmosphere was 75ml/min of N2. The temperature ranges between 100-1000℃ and heating rate was 10℃/min.

2.2.9 Scanning Electron Microscopy (SEM)

Surface morphology of NS admixed cement mortars were analyzed using scanning Electron Microscopy HITACHI Model S-3000H. The Surface morphology of hydrated products obtained by NS admixed with OPC were monitored at lower magnification.

2.2.10 X-Ray Diffraction (XRD)

The evolution of the hydration compounds in cement mortar with NS was evaluated by X-ray diffraction. The cement mortar samples were ground to a particle size lower than 45μm for XRD analysis. XRD measurements were performed on a diffractometer (Philips X'pert) equipped with a graphite monochrometer using Cu-Kα radiation and operating at 40kV and 20mA. Step scanning was made from 5 to 60°-2θ using scan speed of 2°/min and sampling interval of 0.02°-2θ. The XRD patterns are illustrated from 5 to 25°-2θ because more significant peaks of early compounds formed during cement hydration, such as Am (Tri-substituted aluminium ferrite phase) and Calcium hydrates (CH), are detected in this range (Rahhal abd Talero 2005).

2.2.11 FT-IR Spectroscopy

The concrete specimens were broken and the powder sample collected very near to the surface of the rebar were subjected to FT-IR studies using MAKE-BRUKER Optik Gmbh FT-IR spectrometer (Model No-TENSOR27).

3. RESULTS AND DISCUSSION

3.1 Compressive and Split tensile Strength

Table 2 shows the compressive and split tensile strength of NS admixed mortar specimens at 14 and 28 days of curing. The 28 days compressive strength obtained for OPC (Control) mortar was 24.9N/mm^2 and the strength was increased about 1.8 and 2.4 times more than the control at 0.5% NS and 1.0% NS respectively.

OPC mortar showed split tensile strength of 2.76N/mm^2 at 28 days. The addition of NS at 1% level showed a maximum

Table 2. Strength and permeability characteristics of NS dmixed Mortar at 28 days

System	Compressive and Split Tensile strength (N/mm^2)		Charge passed / Coulombs	Steady state diffusion coefficient (m^2sec^{-1})
OPC	32.3	2.76	4110.69	3.69×10^{-12}
OPC+0.5%NS	45.3	2.97	3850.99	2.31×10^{-12}
OPC+1.0%NS	68.2	3.18	3784.21	1.73×10^{-12}
OPC+1.5%NS	58.3	2.97	3487.41	2.77×10^{-12}

split tensile strength of 3.18N/mm^2. Beyond 1% level, the tensile strength decreased. The reactive silica present in NS favoured the formation of Calcium Silicate Hydrate (C–S–H) gel and enhanced the compressive and split tensile strength up to 1.0% level. Above 1.0%, the non–stoichiometric ratio between Ca $(OH)_2$ and SiO_2 decreased the strength values due to the presence of unreactive silica. From the table it was found that the 1.0% NS admixed mortars showed the highest compressive and tensile strength irrespective of curing period. Addition of nano silica accelerates hydration due to chemical reactivity upon dissolution (pozzolanic activity) or to a surface activity which will probably improve the paste – aggregate bond (Nazari and Riahi 2011).

3.2 Rapid Chloride Penetration/Chloride Diffusivity Test

The amount of charge passed and steady state diffusion coefficient at different curing period were reported in Table 2. From the table it was observed that, OPC mortars showed 4110.69 coulombs. The addition of NS considerably reduced the charge passed through the mortar samples. For example 0.5%, 1.0% & 1.5% admixed mortar showed 3850.99, 3784.21 and 3487.41 coulombs respectively. The diffusivity of chloride ions was found to decrease as the curing period increases. The results confirmed that 1.0% NS has lesser diffusion coefficient value when compared to all other systems. NS react with Ca $(OH)_2$ or calcium based phases like aluminates, ferrite and enhanced the C–S–H gel, which interconnected the micro pores present in NS admixed mortars and hence reduced the permeability of chloride. Nano silica fill the voids of the C–S–H gel structure and act as nucleus to tightly with C–S–H gel particles which reduces the calcium leaching rate of cement and therefore increasing their durability(Qing et al. 2007; Gaitero et al. 2008).

3.3. Electrochemical Test

3.3.1 Impressed Voltage Test

The current versus time behaviour of NS admixed mortar systems were illustrated in Fig. 4 From the figure it was found that 0.5 and 1% NS admixed systems have shown lesser anodic current indicating the better performance. At 1.5%, the current was found to be very high but lesser than OPC due to the presence of unreacted silica.

3.3.2 Electrochemical Impedance Spectroscopy (EIS)

Table 3 and Fig. 5 show the impedance parameters R_{ct} and C_{dl} derived from Nyquist plots. The R_{ct} values for steel embedded

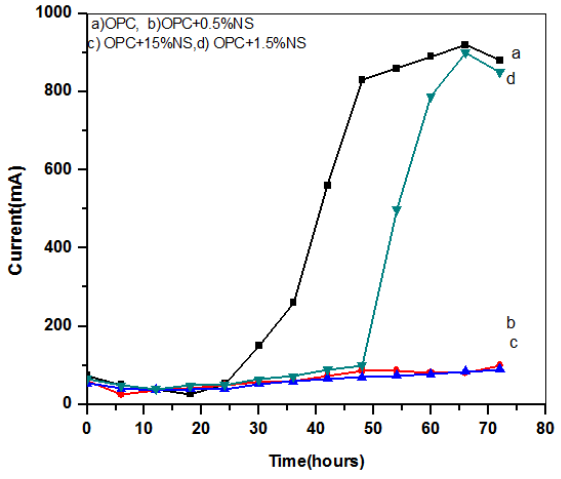

Fig. 4. Current vs. time behavior of NS admixed cement mortar

Table 3. Corrosion kinetic parameters obtained from EIS and Tafel Extrapolation

System	EIS			Tafel Extrapolation		
	I_{corr}	R_{ct}	C_{dl}	E_{corr}	LPR	Icorr
	mA/m^2	Ωm^2	$\times10^{-5}F$	mV	Ωm^2	mA/m^2
OPC	0.170	1.534	5.549	-554.14	2.208	5.557
OPC+0.5%NS	0.100	2.603	6.203	-427.08	3.228	3.424
OPC+1.0%NS	9.984	2.613	6.298	-389.73	3.188	2.078
OPC+1.5%NS	0.162	1.605	7.429	-473.08	2.114	5.217

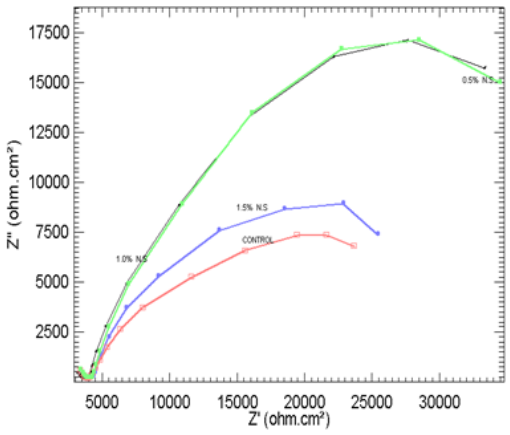

Fig. 5. Impedance spectra of NS admixed cement mortar

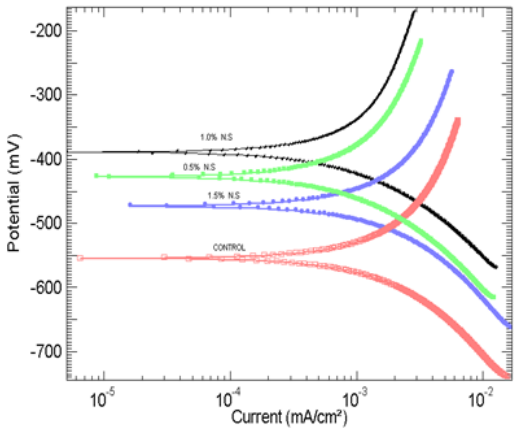

Fig. 6. Tafel Polarization of admixed cement mortar

in 0.5%, 1.0% and 1.5% NS added mortars were found to be 2.603×10^4, 2.613×10^4 and $1.605\times10^4\Omega$. At 0.5 to 1.0%, further in 1.5% NS addition there is a decrease in Rct value observed indicating the optimum percentage. I_{corr} value was also found to be very less for all the NS admixed systems. R_{ct} values increased as the percentage of NS increased. These results confirmed that addition of NS admixed mortar offers more resistance against corrosion than OPC cement mortars.

Similarly the C_{dl} values obtained for OPC mortar was found to be 5.549×10^4. The increase in addition of NS showed increase in C_{dl} values. It is a fact that, a good system must show a greater R_{ct}, C_{dl} values when compared to the respective control system (Muralidharan et al. 2004; Song and Saraswathy, 2006). In this aspect both 0.5% and 1.0% NS systems were found to be more effective in controlling the corrosion of embedded steel.

3.3.3 Tafel Polarization measurements

The corrosion kinetic parameters derived from the potentio-dynamic polarization curves were given in Table 3 and Fig. 6. It was observed from the table that, OPC showed E_{corr} value of −554.14 mV vs. activated titanium. The NS admixed systems showed lesser E_{corr} values. A definite trend was observed between anodic and cathodic Tafel slopes. I_{corr} value for OPC was found to be $5.572\times10^{-4}mA/cm^2$. But all the NS admixed mortars have shown a lesser current density values than the control system.

Among all, 1.0% NS admixed mortar have shown the lesser current density value indicating the better performance. Therefore the systems showing corrosion rate lesser than OPC was considered to be the effective system by improving the corrosion resistance of steel in the presence of aggressive chloride ions (Muralidharan et al. 2004). Interestingly all the NS admixed systems showed corrosion rate lesser than 0.645×10^{-4}mmpy, which represents the better performance by improving the corrosion resistance of steel. Among all, 1.0% NS admixed system was found to be more effective in reducing the self-corrosion of steel in the presence of chloride. The results obtained well agree with EIS measurements.

3.3.4 Thermo Gravimetric Analysis

Typical plots of TG derivative curves for the NS admixed cement mortar exposed after 28 days of curing are given in Fig. 7. Temperature between 450-510℃ is attributed to the dehydration of calcium hydroxide (Vedalakshmi et al. 2009). The main hydrated phases such as Calcium silicate Hydrate (CSH), Calcium Aluminium Silicate Hydrate (C_2ASH) and Calcium Aluminium Hydrate (C_4AH) produced during the pozzolanic was observed between 100 and 600℃.

The sharp endotherm around 465℃ indicates the decom-position of CH formed during hydration. A significant decrease of CH peak was observed at 1.5% NS addition. In the case of 0.5 and 1.0% NS addition the stoichiometric balance of CH and CSH formation was observed from the peak which confirmed

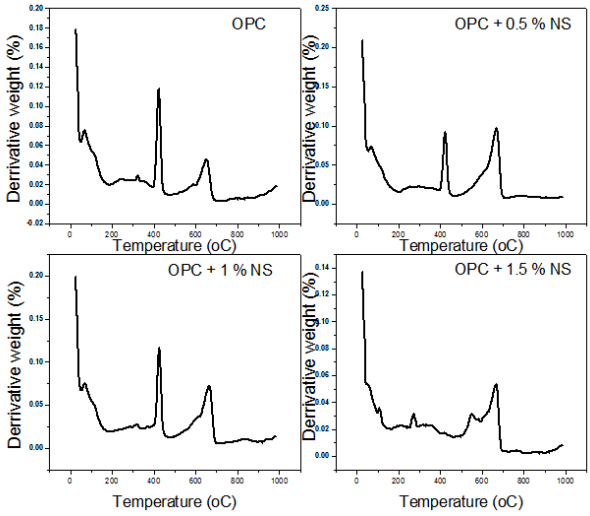

Fig. 7. Derivative TG curves of NS admixed cement mortars

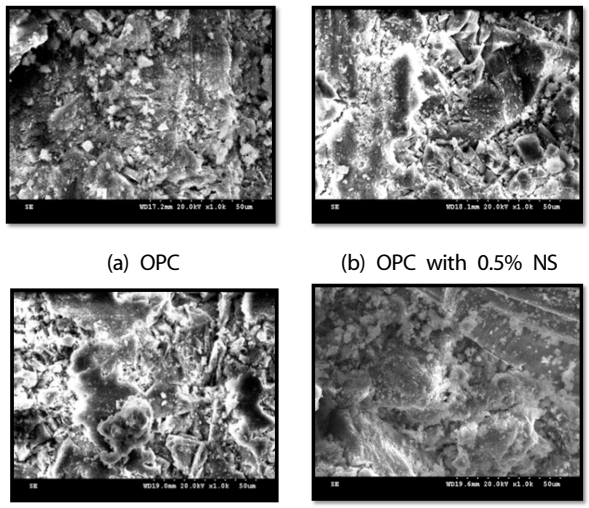

Fig. 8. Nano SiO_2 admixed cement mortars after 28 days

that 1% addition of NS was optimum to increase the mechanical as well as corrosion resistant properties of OPC. Beyond 1% NS, the amount of unreactive NS was increased which reduced further strength enhancement. SiO_2 present in NS reacts with CH form Calcium silicate hydrates (C-S-H) as follows (Qing et al. 2007).

$\equiv Si-O- + H-OH \rightarrow \equiv Si-OH$ (react quickly)

$\equiv Si- + OH \rightarrow \equiv Si-OH$ (react quickly)

$\equiv Si- OH + Ca(OH)_2 \rightarrow C-S-H$

3.3.5 Scanning Electron Microscopy

Fig. 8(a) to 8(d) show the SEM images of nano SiO_2 admixed cement mortars after 28 days of curing. To verify the mechanism predicted by compressive and split tensile test, SEM examinations were performed. Addition of nano-SiO_2 were found to influence hydration behaviour and led to the differences in the micro-structure of hardened cement mortar. NS increases the C-S-H gel and reduced CH formation along with dense, compact and homogeneous structure with crystal formation through the pozzolanic reaction and filler effect of silica particle which is very well evidenced from the SEM images.

3.3.6 XRD

Fig. 9 shows the XRD pattern of different percentage level of NS powder in OPC mortar. The XRD peaks were identified by using JCPDF standard in Table 4. The control system (without NS powder) has shown higher intensity crystal phases such as Calcium Oxide (CaO), Calcium hydroxide ($Ca(OH)_2$) and low intensity crystal phase like calcium silicate (Ca_3SiO_5) calcium aluminum silicate hydroxide hydrate ($CaAl_2Si_2O_7(OH)_2.(H_2O)$)

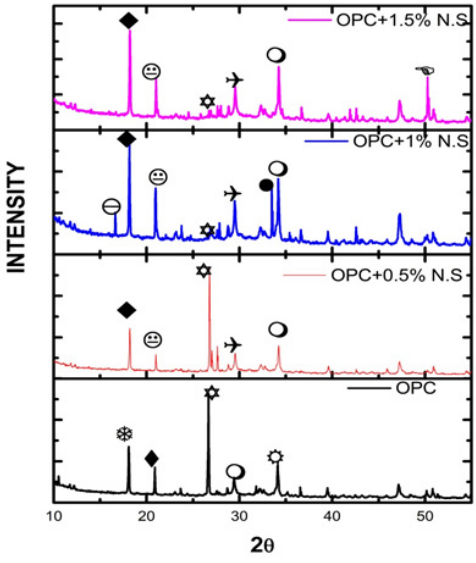

Fig. 9. XRD pattern of OPC and NS admixed mortar

Table 4. XRD results of OPC and NS admixed mortar

d-spacing	Standard d-spacing & PDF number	Compound
5.3201	5.32 (29-0373)	$Ca_2SiO_4.H_2O$ ❖
4.9041	4.9038 (86-0940)	$CaAl_2Si_2O_7(OH)_2.(H_2O)$ ❄
4.8883	4.8880 (41-1420)	$Ca.Al(Si_3.Al)O_8(OH)_4.H_2$ ◆
4.2512	4.2506 (85-1386)	$CaAl_2Si_7O_{18}.(H_2O)_6$ ◆
4.2179	4.2180 (41-1355)	$Ca.Al_2Si_3O_{10}.3H_2O$ ◆
3.332	3.33 (17-0912)	CaO ✡
3.0352	3.036 (42-0551)	$Ca_3Si_iO_5$ ❍
3.0231	3.0235 (72-1396)	$Ca_3(Si_3O_9)$ ×
2.675	2.6758 (46-0341)	$Ca_4Al_8Si_8O32.H_2O$ ●
2.6272	2.6270 (84-1263)	$Ca(OH)_2$ ↺
2.6194	2.619 (14-0693)	Ca_3SiO_5 ❍
1.814	1.8136 (82-0511)	SiO_2 ☜

and calcium aluminum silicate hydrate ($CaAl_2Si_7O_{18}.(H_2O)_6$). While 0.5% of NS addition resulted in an increase of crystal phase like calcium silicate ($Ca_3(Si_3O_9)$ and Ca_3SiO_5), calcium aluminum silicate hydroxide hydrate ($Ca \cdot Al(Si_3 \cdot Al)O_8(OH)_4 \cdot H_2O$) and calcium aluminum silicate hydrate ($Ca \cdot Al_2\ Si_3O_{10} \cdot 3H_2O$). 1.0% NS powder has shown to reduce crystal phases of calcium oxide peak and calcium hydroxide peak when compared to the other systems. The formation of calcium silicate hydrate ($Ca_2SiO_4 \cdot H_2O$), calcium silicate (Ca_3SiO_5 and $Ca_3(Si_3O_9)$, calcium aluminum silicate hydroxide hydrate ($Ca \cdot Al(Si_3.Al)O_8(OH)_4 \cdot H_2O$) and calcium aluminum silicate hydrate ($Ca \cdot Al_2Si_3O_{10} \cdot 3H_2O$ and $Ca_4Al_8Si_8O_{32} \cdot H_2O$) are gradually increased with crystal phase peaks were noticed. It is clearly understood that NS reacted with $Ca(OH)_2$ to form calcium silicate (Ca_3SiO_5 and $Ca_3Si_3O_9$) or calcium aluminum silicate hydroxide hydrate ($Ca \cdot Al(Si_3 \cdot Al)O_8(OH)4 \cdot H_2O$) and calcium aluminum silicate hydrate ($Ca \cdot Al_2Si_3O_{10} \cdot 3H_2O$ and $Ca_4Al_8Si_8O_{32} \cdot H_2O$) crystal phase, which resultant to reduce the calcium oxide and calcium hydroxide peak. Naji et al. (2011) have reported the same observation in which lime reacts NS particles causes more C-S-H gel, when cured in lime solution. The content of C-S-H gel is increased because of high free energy of nano-particles which reduces significantly when reacts with $Ca(OH)_2$ (Naji et al. 2011). Similar crystal phase peaks were noticed in 1.5% NS powder in OPC cements, in addition to this unreacted or free nano silica are represented in XRD peaks. From this result it is clearly indicated that 1.0% of NS addition is found to be the tolerable limit in OPC cement mortar.

3.3.7 Fourier Transform Infrared Spectroscopy

Concrete samples were characterized by FT-IR, after completion of the experiments. Three types of samples were analyzed such as OPC, OPC with 0.5 and 1.0% NS addition in cement mortar. Fig. 10 shows the detail about FT-IR peaks. The peaks were detected in the range of 3700-3000 and 1700-450. Portlandite is barely detected at 3640cm^{-1} due to the OH stretching vibration; the attribution of this peak is well referenced in literature (Amboise et al. 1994; Chollet and Horgnies 2011). Secondly, the major peaks are at 1100 and 974cm^{-1} in the characteristic of SiO_4 and CSH stretching vibration (Yu et al. 1999). The broad peak around 3404cm^{-1} is assigned to the stretching vibration of the OH band from residual water(Gao et al. 1999). Whereas in 1% NS, CO stretching reduced because nanosilica react with calcium carbonate in the range of 1490cm^{-1}.

Increased CSH formation resulted in an increase in strength and reduced diffusion coefficient due to the pore size refinement is very well evidenced from FTIR results.

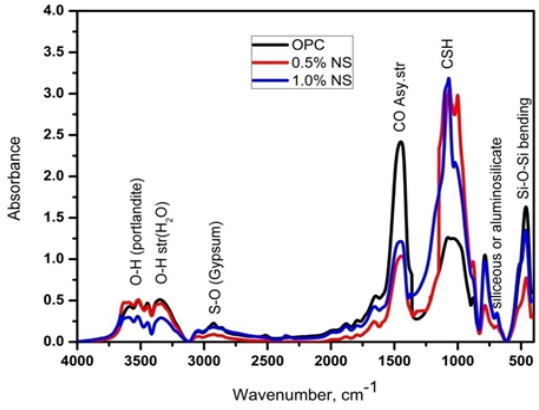

Fig. 10. FT-IR pattern of OPC and NS admixed cement mortar

4. CONCLUSIONS

The following conclusions were drawn from the above investigation:

1% NS addition shows higher compressive and split tensile strength due to accelerated hydration process, reduced chloride diffusivity and better corrosion resistance properties due to the formation of dense and compact formation of C-S-H gel. SEM images revealed that NS consumes CH crystals, decreases the orientation of CH crystals, reduces the size of CH crystals and improves the interface structure more effectively than OPC. Therefore the results indicate that nano scale silica behaves not only as a filler to improve microstructure, but also as an activator to promote pozzolanic reaction. XRD and FT-IR results confirm that 1% NS addition was found to be the tolerable limit. Hence 1% NS may be recommended for making high performance concrete applications.

ACKNOWLEDGEMENTS

This research was supported by Basic Science Research Program through the National Research Foundation of Korea (NRF) funded by the Ministry of Education (NRF-2013R1A1A2060114).

REFERENCES

Amboise, J., Maximilien, S., Pera, J. (1994). Properties of metakaolin blended cements, Advanced Cement Based Materials, **1(4)**, 161-168.

Amutha, K., Ravibaskar, R., and Sivakumar, G. (2010). Extraction, synthesis and characterization of nano silica from rice husk ash International Journal of Nanotechnology & Applications. **4(1)**, 61-66.

Bjornstrom, J., Martinelli, A., Matic, A., Borjesson, L., and Panas, I. (2004). Accelerating effects of colloidal nano-silica for beneficial calcium silicate hydrate formation in cement, Chemical Physics Letters, **392(1-3)**, 242-248.

Chen, R.S. and Ye, Q. (2002), Preliminary study on the water permeability and microstructure of concrete incorporating nano-SiO_2, Concrete, **1**, 7-10.

Chollet, M. and Horgnies, M. (2011). Analyses of the surfaces of concrete by Raman and FT-IR spectroscopies: comparative study of hardened samples after demoulding and after organic post-treatment, Surface and Interface Analysis, **43(3)**, 714-725.

Constantinides, G. and Ulm, F.J. (2004). The effect of two types of C-S-H on the elasticity of cement- based materials: Results from nano indentation and micromechanical modeling, Cement and Concrete Research, **34(1)**, 67-80.

Gaitero, J.J., Campillo, I., and Guerrero, A. (2008). Reduction of the calcium leaching rate of cement paste by addition of silica nanoparticles, Cement and Concrete Research, **389(8-9),** 1112-1118.

Gao, X.F., Lo, Y., Tam, C.M., and Chung, C.Y. (1999). Analysis of the infrared spectrum and microstructure of hardened cement paste, Cement and Concrete Research, **29(6)**, 805-812.

Givi, A.N., Rashid, S.A., Aziz, F.N.A., and Salleh, M.A.M. (2011). The effects of lime solution on the properties of SiO_2 nanoparticles binary blended concrete, Composites Part B : Engineering, **42(3)**, 562-569.

Gonen, T. and Yazicioglu, S. (2007). The influence of mineral admixtures on the short and long-term performance of concrete, Building and Environment, **42(8)**, 3080-3085.

Hassan, K.E., Cabrera, J.G., and Maliehe, R.S. (2000). The effect of mineral admixtures on the properties of high-performance concrete, Cement and Concrete Composites, **22(4)**, 267-271.

Ji, T. (2005). Preliminary study on the water permeability and microstructure of concrete incorporating nano-SiO_2, Cement and Concrete Research, **35**, 1943-1947.

Khanzadi, M., Tadayon, M., Sephri, H., and sepehri, M. (2010). International conference on sustainable construction materials and technologies, Universita Polilencnica delle Marche, Ancona Italy.

Li, G. (2004). Properties of high-volume fly ash concrete incorporating nano-SiO_2, Cement and Concrete Research, **34(6),** 1043-1049.

Li, H., Xiao H., Yuan, J., and Ou, J. (2004). Microstructure of cement mortar with nano- particles, Composites Part B: Engineering, **35(2)**, 185-189.

Lin, K.L., Chang, W.C., Lin, D.F., Luo, H.L., and Tsai, M.L. (2008). Effects of nano-SiO_2 and different ash particle sizes on sludge ash-cement mortar, Journal of Environmental

Management, **88(4),** 708-714.

Memon, H., Radin, S.S., Zain, M.F.M., Trottier, and Jean-Francois. (2002). Effects of mineral and chemical admixtures on high-strength concrete in seawater, Cement and Concrete Research, **32(3),** 373-377.

Mondal, P., Shah, S.P., Marks, L.D., and Geitero, J.J. (2010). Comparative study of the effects of microsilica nanosilica in concrete, Journal of the Transportation Research Board, **2141(1)**, 6-9.

Muralidharan, S., Saraswathy, V., Merlin Nima, S.P., and Palaniswamy, N. (2004). Evaluation of a composite corrosion inhibiting admixtures and its performance in Portland pozzolana cement, Materials Chemistry and Physics, **86(2)**, 298-306.

Naji, A., Abdul, S., Nora, F., Aziz, A., Amran, M., and Salleh, M. (2011). The effect of lime solution on the properties of SiO_2 nanoparticels binary blended concrete, Composites part B: Engineering, **42(3)**, 562-569.

Nazari, A. and Riahi, S. (2011). The Effects of ZnO_2 Nano particles on properties of concrete using ground granulated blast furnace slag as binder, Materials Research, **14(3)**, 299-306.

Qing, Y., Zenam, Z., Deyu, K., and Rongshen, C. (2007). Influence of nano-SiO_2 addition on properties of hardened cement paste as compared with silica fume, Construction and Building Materials, **21(3)**, 539-545.

Rahhal, V. and Talero, R. (2005). Early hydration of Portland cement with crystalline mineral additions, Cement and Concrete Research, **35(7)**, 1285-1291.

Ranjbar, Z. and Rastegar, S. (2009). The influence of surface chemistry of nano-silica on microstructure, optical and mechanical properties of the nano-silica containing clear-coats, Progress in Organic Coatings, **65(1)**, 125-130.

Senff, L., Labrincha, J.A., Ferreira, V.M., Holza, D., and Repette, W.L. (2009), Effect of nano-silica on rheology and fresh properties of cement pastes and mortars, Construction and Building Materials, **23(7)**, 2487-2491.

Shannag, M.J. (2011), Characteristics of lightweight concrete containing mineral admixtures, Construction and Building Materials, **25(2)**, 658-662.

Sobolev, K. and Ferrara, A. (2005), How nanotechnology can change the concrete word, American Ceramic Bulletin, **84(10)**, 15-17.

Song, H.W. and Saraswathy, V. (2006), Analysis of corrosion resistance behavior of inhibitors in concrete using electro-chemical techniques, Metals and Materials International, **12(4)**, 323-329.

Tasdemir, C. (2003), Combined effects of mineral admixtures and curing conditions on the sorptivity coefficient of concrete, Cement and Concrete Research, **33(10)**, 1637-1642.

Vedalakshmi, K., Saraswathy, V., Song, H.W., and Palaniswamy, N. (2009), Determination of diffusion coefficient of chloride in concrete using Warburg diffusion coefficient, Corrosion Science, **51(6)**, 1299-1307.

Ye, Q. (2001), Research on the comparison of pozzolanic activity between nano SiO_2 and silica fume, Concrete, **3**, 19-22.

Ye, Q., Zhang, Z.N., Chen, R.S., and Ma, C.C. (2003), Interaction of nano-SiO_2 with calcium hydroxide crystals at interface between hardened cement paste and aggregate, Journal of the Chinese Ceramic Society, **31(5)**, 517-522.

Yu, P., Kirkpatrick, R.J., Poe, B., McMillan, P.F., Cong, X. (1999), Structure of calcium silicate hydrate (C-S-H) near-Mid-and far Infrared Spectroscopy, Journal of the American Ceramic Society, **82(3)**, 742-748.